Electronic Supplementary Material (ESI) for Physical Chemistry Chemical Physics.

Supplementary Information: Phase coherent excitation of SABRE permits simultaneous hyperpolarization of multiple targets at high magnetic field

Jacob R. Lindale[a], Shannon L. Eriksson[a,b], Warren S. Warren[c]

[a] Department of Chemistry, Duke University, Durham, NC, 27708. [b] School of Medicine, Duke University, Durham, NC, 27708. [c] Departments of Physics, Biomedical Engineering, and Radiology, Duke University, Durham, NC, 27708.

^{1}H decoupled LIGHT-SABRE simulations

The broadband X-SABRE experiment introduced here is only the second experiment to generate hyperpolarization in asymmetric ligand environments at high field. Comparing its performance to the ^{1}H decoupled LIGHT-SABRE (^{1}H dLIGHT) experiment(1) (**Fig. S1**) provides insight on the various benefits of this method. The pulse sequence parameter space for the ^{1}H dLIGHT experiment spans several parameters, such as the SLIC-pulse length t_p, the exchange delay t_d, the SLIC pulse power $\omega_{1,N}$ and resonance offset $\Delta\omega_N$, and the ^{1}H decoupling power $\omega_{1,H}$. As both of these experiments were benchmarked on the ^{15}N-acetonitrile/^{14}N-pyridine X-SABRE complex, we will use simulations of this system also as a reference. We will fix ^{1}H decoupling power at the experimentally optimized $\omega_{1,H} = 1.6\ kHz$.

This phase space may be efficiently explored *in silico* with the DMExFR2(2) simulation package built and experimentally verified for SABRE. Broadly, we find that hyperpolarization is optimized for $t_d = 0\ ms$, i.e. continuously irradiating on both ^{1}H and ^{15}N at the respective conditions. This significantly reduces the size of the parameter phase space that must be searched to $\omega_{1,N}$ and $\Delta\omega_N$, which is shown in **Fig. S2** for $k_N = 16\ s^{-1}$ and $k_N = 150\ s^{-1}$. The position of the optimum is marked by the solid crosshairs and the position of the level anti-crossing (LAC) predicted optimum is shown with the dashed crosshair. These pulse sequence parameters were used to generate the exchange rate dependent simulations shown in **Fig. 4** in the main text.

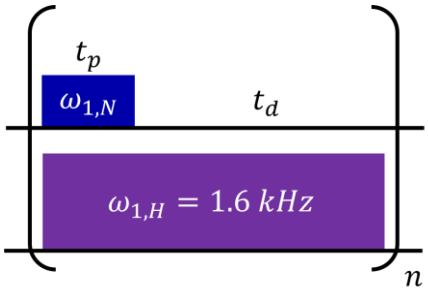

Fig. S1 ^{1}H decoupled LIGHT-SABRE experiment. Continuous irradiation on ^{1}H preserves the $\hat{I}_1 \cdot \hat{I}_2$ spin order and permits SLIC-based hyperpolarization methods in asymmetric ligand environments. For ^{15}N-acetonitrile at 8.45T, $\omega_{1,H} = 1.6\ kHz$ was experimentally optimized and is used in all of the following simulations.

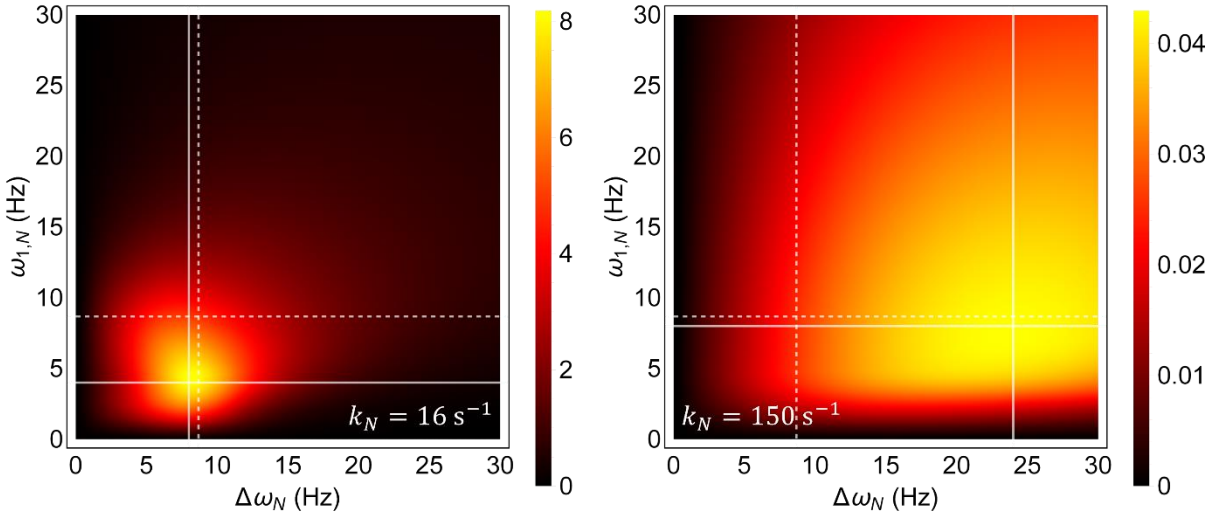

Fig S2 Optimization of ^{1}H decoupled LIGHT-SABRE simulations for ^{15}N-acetonitrile at 8.45T. For these simulations, $k_H = 2\ s^{-1}$, $\omega_{1,N} = 1.6\ kHz$, and $[Ir]/[S] = 1/20$. All simulations were run for 20s. The positions of the optimum conditions are indicated by solid crosshairs. The dashed crosshairs indicate the condition predicted by the level anti-crossing, which is $\Delta\omega_N \approx \omega_{1,N} \approx J_{HH}$. Notably, the optimal hyperpolarization conditions are found at positions that are nearly a factor of two different from the LAC prediction for both cases.

Refocusing the τ_{HH} delay

The broadband X-SABRE experiment utilizes phase cycling to remove the effects of $\hat{\mathcal{H}}_Z$, which manifests as oscillatory structures in both $\Delta\omega_N$ and τ_{HH}. A pair of 180_y pulses (or other phases) may be added to the pulse sequence at $\tau_{HH}/2$ to refocus evolution under $\hat{\mathcal{H}}_Z$, which theoretically should greatly simplify the experiment and remove the need for phase cycling (**Fig. S3A**). However, this changes the net flip angle of the experiment to $(2n+1)\pi$ and has the effect that it inverts the hyperpolarization with each successive application of the pulse sequence. Refocusing the τ_{HH} delay does, in fact, remove the oscillatory structure from the $\Delta\omega_N$ and τ_{HH} profiles, but greatly reduces the resultant hyperpolarization under this pulse sequence (**Fig. S3B**).

Notably, evolution under $\hat{\mathcal{H}}_Z$ will have an adverse effect when hyperpolarizing in strongly inhomogeneous fields, as phase cycling will not be able to compensate for the inhomogeneities. However, the experiments here were performed with continuous parahydrogen bubbling at 8.45T, where the large susceptibility difference between the gaseous and liquid phases generates large inhomogeneities which are most prominent on the ^{1}H channel. Even still, hyperpolarization was readily achieved with this pulse sequence.

Simulation parameters

The ^{15}N-acetonitrile system was characterized at 8.45T, and the key parameters for this system are given here in detail. The Hamiltonian of this system is:

$$\begin{aligned}\hat{\mathcal{H}} = \Delta\omega_{HH}(\hat{I}_{1z} - \hat{I}_{2z}) + \omega_{Hm}\sum_{i=1}^{3}\hat{I}_{iz} \\ +2\pi\left(J_{HH}\hat{I}_1\cdot\hat{I}_2 + J_{NH}\hat{I}_{1z}\hat{S}_z\right) \\ +2\pi J_{NHm}\sum_{i=1}^{3}\hat{I}_{iz}\hat{S}_z\end{aligned} \qquad (S1)$$

The parameters ω_{Hm} and J_{NHm} are the precession frequencies of the methyl ^{1}H and the J-coupling to these nuclei from the ^{15}N spin. We have assumed the same

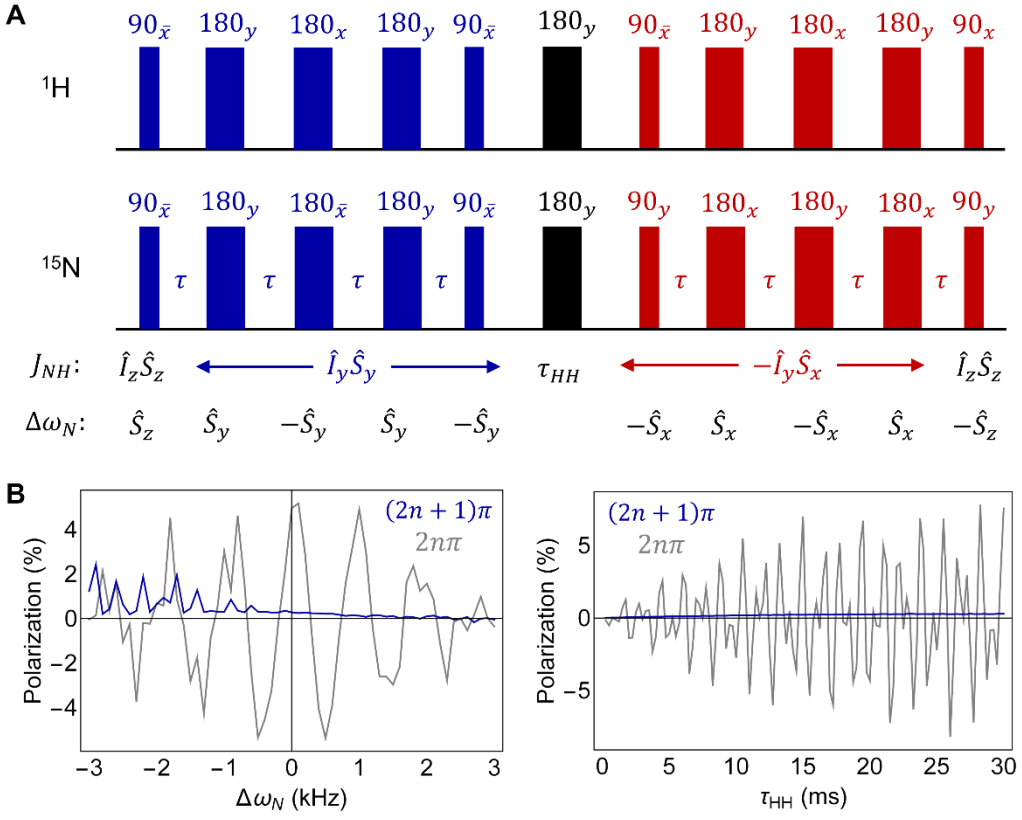

Fig. S3 τ_{HH} refocused version of the broadband X-SABRE experiment. **A.** Evolution under $\hat{\mathcal{H}}_Z$ may be refocused by adding two 180_y pulses at $\tau_{HH}/2$. The significant difference in this sequence compared to the non-refocused version is that the net flip angle of this sequence is $(2n+1)\pi$ whereas the non-refocused version has a net flip angle of $2n\pi$. **B.** While the dependence on the resonance offset and τ_{HH} no longer have oscillatory structures due to the refocusing of $\hat{\mathcal{H}}_Z$, the resultant hyperpolarization is significantly lower over the entire pulse sequence. For the $\Delta\omega_N$ profile, $\tau_{HH} = 21\ ms$ and for the τ_{HH} scan, $\Delta\omega_N = 0\ Hz$. For all simulations, $\tau = 3\ ms$, $k_N = 16\ s^{-1}$, $k_H = 2\ s^{-1}$, and $[Ir]/[S] = 1/20$.

rotating frame as used in eq. 2 with $\Delta\omega_N = 0$ and have dropped the pulses for brevity. The numerical values of these parameters are:

$$\Delta\omega_{HH} = 460\ Hz \qquad (S2a)$$

$$\omega_{Hm} = 10\ kHz \qquad (S2b)$$

$$J_{NH} = -25.41\ Hz \qquad (S2c)$$

$$J_{HH} = -8.68\ Hz \qquad (S2d)$$

$$J_{NHm} = -1.69\ Hz \qquad (S2e)$$

For the simulations fit to the experimental data, there was a $\Delta\omega_H = -734\ Hz$ and $\Delta\omega_{N,b} = 935\ Hz$ resonance offset for the bound species and $\Delta\omega_{N,f} = -857$ offset for the free ^{15}N species.

Signal-to-noise calculations in multicomponent spectrum

The signal-to-noise of each of the components in the spectrum shown in **Fig. 8C** is plotted in **Fig. S4** relative to its concentration. This suggests that there is limited competition for binding the iridium complex in this mixture of analytes, which may be facilitated by the vast number of binding geometries that are available with multiple components.

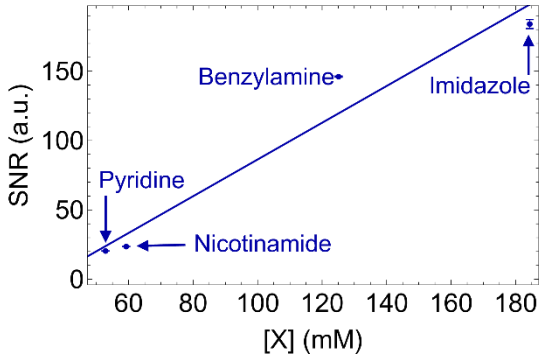

Fig. S4 Signal to noise of various components (X) as a function of their concentration ([X]). A linear fit to the data is shown, having a $R^2 = 0.98$.

Fine sampling of broadband resonance profile

The field profile of the broadband X-SABRE experiment shown here was sampled at a rate higher than the Nyquist rate of the structures to highlight the fine structure (Fig. S5). The fine structure of this profile primarily arises from evolution under the Zeeman Hamiltonian during τ_{HH} delay. Under sampling this profile generates structure at a multiple of the frequency structure of this plot, which is observed in Fig. 5.

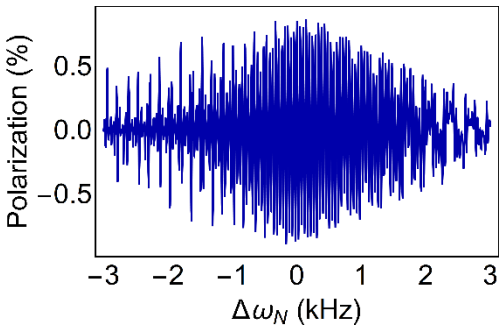

Fig. S5 Fine sampling of the broadband X-SABRE profile. We see fine structure arising from evolution under the Zeeman Hamiltonian during the τ_{HH} delay. Down-sampling this structure creates the oscillatory structure observed in Fig. 5.

References

1. Lindale JR, Tanner CPN, Eriksson SL, & Warren WS (2019) Decoupled LIGHT-SABRE variants allow hyperpolarization of asymmetric SABRE systems at an arbitrary field. *Journal of Magnetic Resonance* 307:106577.
2. Lindale JR, Eriksson SL, Tanner CPN, & Warren WS (2020) Infinite-order perturbative treatment for quantum evolution with exchange. *Science Advances* 6(32):eabb6874.